Z. Stuchlík, G. Török, V. Karas and D. Lančová, editors, Silesian University in Opava, 2023, pp. 47–53

Energy spectrum of ultra high energy cosmic rays accelerated by rotating supermassive black holes

Martin Kološ[1,a] and Arman Tursunov[2,1,b]

[1]Institute of Physics, Silesian University in Opava,
Bezručovo nám.13, CZ-74601 Opava, Czech Republic
[2]Max Planck Institute for Radio Astronomy,
Auf dem Hügel 69, Bonn D-53121, Germany
[a]martin.kolos@physics.slu.cz
[b]arman.tursunov@physics.slu.cz

ABSTRACT
We explore the acceleration of charged particles in the combined gravitational and magnetic field around a rotating Kerr black hole. We derive the energy spectrum for ionized particles escaping to infinity, which can serve as injection spectrum for observed ultra-high energy cosmic rays.

Keywords: Black hole – resonances – particle dynamics – magnetic field

1 INTRODUCTION

Rotating black holes (BHs) are likely the largest energy reservoirs in the Universe as predicted by BH thermodynamics, while cosmic rays (CRs) are the most energetic among particles detected on Earth. Magnetic fields surrounding BHs combined with strong gravity effects, thanks to the spacetime symmetries, turn the BHs into powerful accelerators of charged particles (Kardashev, 1995). At the same time, in the age of multi-wavelength and multi-messenger astronomy, BHs and their environments have not yet been probed with CR messengers despite being observed across most of the electromagnetic spectrum, neutrino and gravitational waves.

The production and acceleration mechanisms of ultra-high-energy cosmic rays (UHECRs) of energy $> 10^{20}$eV, beyond the GZK-cutoff limit remain unclear and point to the exotic nature of the phenomena. Recent observations of extragalactic neutrinos may indicate that the source of UHECRs is an extragalactic supermassive black hole (SMBH). Tursunov et al. (2020) have shown that SMBH can efficiently accelerate UHECR protons through the extraction of rotational energy of SMBH in the presence of an external magnetic field. Applying to a larger number of SMBH candidates in the centers of active galactic nuclei (AGN) in the local universe, Tursunov et al. (2022) have found that the mean energy of primary cosmic rays in most AGN sources is roughly of or above the order of

978-80-7510-577-6

the spectral ankle – a flattening of the slope of the cosmic-ray spectrum measured around $10^{18.6}$ eV energy. Therefore, local SMBH can provide a sufficient contribution to the ankle and observed all-particle spectrum, which necessitates further analysis of the model and prediction of the energy spectrum of accelerated particles from SMBH, taking into account the dynamic surroundings of AGN.

2 ELECTROMAGNETIC FIELD AROUND ROTATING BLACK HOLE

When the magnetic field surrounding a black hole is weaker than $B \ll B_{\rm G} = 10^{19}(M_{\odot}/M)$ Gs, its contribution to background spacetime geometry is negligible, and the geometry of the rotating black hole is given the Kerr metric

$$\mathrm{d}s^2 = g_{tt}\mathrm{d}t^2 + 2g_{t\phi}\mathrm{d}t\mathrm{d}\phi + g_{\phi\phi}\mathrm{d}\phi^2 + g_{rr}\mathrm{d}r^2 + g_{\theta\theta}\mathrm{d}\theta^2, \tag{1}$$

with the nonzero components of the metric tensor taking in the standard Boyer-Lindquist coordinates the form

$$\begin{aligned} g_{tt} &= -\left(1 - \frac{2Mr}{\Sigma}\right), \quad g_{rr} = \frac{\Sigma}{\Delta}, \quad g_{\theta\theta} = \Sigma, \quad g_{t\phi} = -\frac{2Mra\sin^2\theta}{\Sigma}, \\ g_{\phi\phi} &= \left(r^2 + a^2 + \frac{2Mra^2}{\Sigma}\sin^2\theta\right)\sin^2\theta, \end{aligned} \tag{2}$$

where $\Sigma = r^2 + a^2\cos^2\theta, \quad \Delta = r^2 - 2Mr + a^2$. Here, M is the gravitational mass of the black hole, and a is its spin parameter.

Due to the stationarity and axial symmetry of the Kerr black hole spacetime, the four-vector potential of the weak magnetic field introduced by Wald (1974), which is the solution of the vacuum Maxwell equations, takes the form

$$A_t = \frac{B}{2}\left(g_{t\phi} + 2ag_{tt}\right), \quad A_\phi = \frac{B}{2}\left(g_{\phi\phi} + 2ag_{t\phi}\right). \tag{3}$$

The terms proportional to the rotation parameter a contribute to Faraday induction, which generates an electric potential producing an induced electric field (Wald, 1974). The potential difference between the horizon of a black hole and infinity takes the form

$$\Delta\varphi = \varphi_{\rm H} - \varphi_\infty = \frac{Q - 2aMB}{2M}. \tag{4}$$

This causes a selective accretion of charged particles into the rotating black hole. The process is similar to the field generated by the rotating conductor immersed in a magnetic field.

Thus, the expressions (3) for the non-zero covariant components of the four-vector potential have to be rewritten as (Tursunov et al., 2016)

$$A_t = \frac{B}{2}\left(g_{t\phi} + 2ag_{tt}\right) - \frac{Q}{2M}g_{tt}, \quad A_\phi = \frac{B}{2}\left(g_{\phi\phi} + 2ag_{t\phi}\right) - \frac{Q}{2M}g_{t\phi}. \tag{5}$$

The process of selective accretion for astrophysical black holes surrounded by plasma occurs in very short timescales, until the potential difference vanishes, which means that the

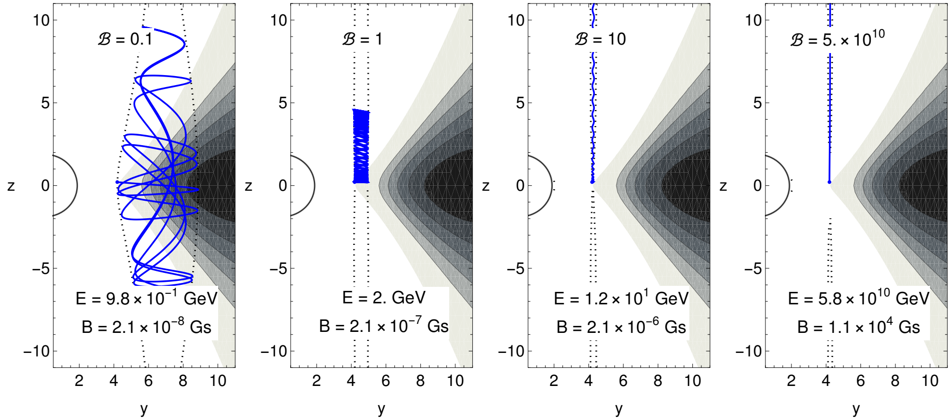

Figure 1. Examples of ionized charged particle trajectories around magnetized rotating Kerr SMBH ($M = 10^8 M_\odot, a = 0.5$). The solid blue curves represent a projection of the particle's trajectory into the x-z plane, and the dotted lines show the boundaries of the motion given by the combined effect of gravity and magnetic field. The black circle represents the BH horizon, and a cross-section of the accretion torus is plotted with different shades of grey. If the electromagnetic field influence (EFI) is small or comparable with gravity ($\mathcal{B} = 0.1$ and $\mathcal{B} = 1$), the charged particle is bounded by the gravitational potential of BH. In this case, we observe a rich, chaotic dynamic; if EFI slightly dominates over gravity ($\mathcal{B} = 10$), the particle predominantly orbits along magnetic field lines; and finally, if EFI is much stronger than gravity ($\mathcal{B} = 5 \cdot 10^{10}$), the charged particle flies away with the γ-factor proportional to the parameter $\mathcal{B}$.

black hole acquires an induced electric charge $Q_\mathrm{W} = 2aMB$. Despite the classical screening effect of plasma, it has been shown by Komissarov (2022) that the induced electric field of a black hole cannot be shielded, at least within the ergosphere. The role of this charge and its possible observational test were discussed by Zajaček et al. (2018) for the Galactic centre SMBH. The value of the Wald charge $Q_\mathrm{W} = 2MaB \leq 2M^2 B$ is

$$Q_\mathrm{W} \leq 10^{14} \left(\frac{M}{M_\odot}\right)^2 \left(\frac{B}{10^4\mathrm{Gs}}\right) \mathrm{statC}, \tag{6}$$

which is weak in the same sense as the external magnetic field, that is, it cannot modify the background geometry of the black hole.

Despite the weakness of the electromagnetic field for spacetime curvature, in astrophysical conditions, its effect is non-negligible for the motion of charged particles, such as electrons and ions. The relative influence of magnetic and gravitational forces is governed by the specific charge of the particle (ratio of the electric charge to mass of the particle) and is of the order of (Frolov and Shoom, 2010)

$$b \sim 4.7 \times 10^7 \left(\frac{q}{e}\right)\left(\frac{m}{m_\mathrm{p}}\right)^{-1} \left(\frac{B}{10^8\mathrm{Gs}}\right)\left(\frac{M}{10 M_\odot}\right), \tag{7}$$

where m_p is the proton mass.

3 ENERGY SPECTRUM OF IONIZED ACCELERATED PARTICLES

Black holes can accelerate particles through the Penrose process (Penrose and Floyd, 1971), where an initial particle splits in the ergosphere of the rotating Kerr black hole into two fragments. If one of the secondary particles, after splitting, attains negative energy with respect to an observer at infinity, it will inevitably be captured by the black hole. Thanks to the energy conservation law, the second fragment gets a chance to escape to infinity with energy greater than that of the initial particle. Such an energy gain occurs at the expense of the black hole's rotational energy. For neutral particles, the increase in energy per particle is limited to $\eta = 0.21$. However, the inclusion of an electromagnetic interaction into the Penrose process changes the situation dramatically (Wagh et al., 1985; Stuchlík and Kološ, 2016; Dadhich et al., 2018; Tursunov et al., 2021). In the magnetic Penrose process (MPP) (Wagh et al., 1985), the charged particles can increase their energies by the factor even exceeding $\eta = 10^{12}$ (Tursunov et al., 2020; Tursunov and Dadhich, 2019; Tursunov et al., 2022). Moreover, in contrast to the neutral version, in MPP, the acceleration zone goes far beyond the ergosphere (a region with negative energy orbits of neutral particles) to an effective ergoregion (a region with negative energy orbits of neutral particles).

In the MPP ionization process, a neutral particle 1 splits into two oppositely charged particles – 2 and 3, with charges q_2 and q_3, respectively. The conservation of the electric charge and canonical momentum gives

$$0 = q_2 + q_3 \quad \pi_{\alpha(1)} = \pi_{\alpha(2)} + \pi_{\alpha(3)}, \tag{8}$$

where $\pi_{\alpha(i)}$, $i = \{1, 2, 3\}$ denotes the canonical momentum of 1st, 2nd and 3rd particles, respectively. Due to the charge conservation, the momentum conservation from Eq. (8) takes the form

$$p_{\alpha(1)} = p_{\alpha(2)} + q_2 A_\alpha + p_{\alpha(3)} + q_3 A_\alpha = p_{\alpha(2)} + p_{\alpha(3)}. \tag{9}$$

In physical scenarios, ionized particles are much more massive than electrons, i.e., $m_2/m_3 \gg 1$, as in the case of ionization of neutral atoms. The time component of the canonical momentum gives the energy of the particle with respect to the distant observer $E = -\pi_t$. As we can see from Eq. (8), the accelerated particle is gaining energy mostly through qA_t term, and if the electromagnetic interaction is strong enough, the particle's momentum can be neglected

$$E \sim qA_t(r, \theta). \tag{10}$$

One can estimate the maximal energy of an escaping particle (for example, a proton) from supermassive BH with the realistic magnetic field

$$E_\mathrm{p} = 1.7 \times 10^{11}\,\mathrm{GeV} \left(\frac{q}{e}\right)\left(\frac{m_p}{m}\right)\left(\frac{B}{10^4\mathrm{Gs}}\right)\left(\frac{M}{10^9 M_\odot}\right)\left(\frac{a}{0.8}\right), \tag{11}$$

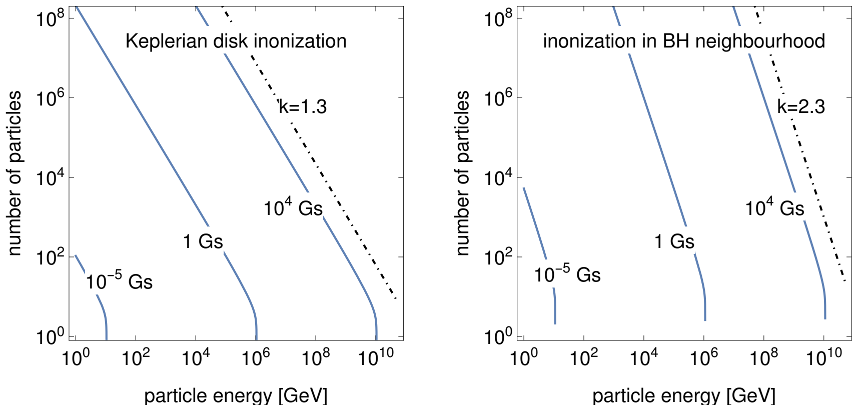

Figure 2. Distribution of accelerated particles as a function of energy for cosmic rays accelerated by SMBHs ($M = 10^8 M_{\rm sun}$) in a magnetic field with various strengths. The BH is rotating with $a = 0.5$ spin parameter, and the ionization probability is $\epsilon = 1$ for the proton. Both models for particle distribution in the Keplerian disk (left) and in the volume of the black hole's environment (right) are presented. The spectral index k is sensitive to the initial distribution of the particle. The sudden drop in the number of particles with higher energies is caused by the truncation of the particle distribution at the innermost edge of the accretion disk.

predicting energy of proton $E_{\rm p}$ exceeding 10^{11} GeV for $M \sim 10^9 M_\odot$ and $B \sim 10^4$Gs (Tursunov et al., 2022). Presented MPP acceleration scenario for BHs, belong to "one-shot" models as classified in Rieger (2022).

An example of charged particle trajectories can be found in Fig. 1, where the trajectory for ultra-high energy particles is plotted. As one can see from Eq. 11, rotating supermassive BHs can accelerate charged particles to the highest observed UHECR, or even higher. To check the validity of UHECR production through MPP, one needs to find the UHECR energy spectrum, giving the number of particles N per energy E, that particle energy spectrum $N = N(E)$ (Rieger, 2022).

The toy model for the particle energy distribution function $N(E)$ can be obtained from the analogy of a black hole as a point charge Q accelerating test particle of charge q. The electrostatic potential energy for such a system from a classical physics viewpoint is proportional to both charges and inversely proportional to the distance $E \sim qQ/r$. We assume that the total number of particles in the volume of a radius r is proportional to the number of accelerated ionized particles, so that $N \sim r^3$. One can write particle energy spectrum

$$N = N_0 E^k, \tag{12}$$

where the spectral index k is $k = 3$. For a rotating black hole in a magnetic field, a more sophisticated model can be constructed, although the spectral index has to remain in the range $k \in (1, 3)$.

Let us assume that the accretion disk of a black hole is located mostly in the equatorial plane and that the probability of neutral particle ionization is proportional to the particle density $\sigma(r)$ and the temperature profile $T(r)$ of the accretion disk. This gives

$$N(r) = \epsilon\, r^2\, \sigma(r)\, T(r), \tag{13}$$

where ϵ is a dimensional constant representing the probability of the ionization process. The energy of a charged particle after the MPP ionization process is

$$E(r) \approx qA_t(r, \pi/2) \approx -\frac{q\, 2aB}{r}, \tag{14}$$

which is an electrostatic energy between the charge q of the particle and that of the Wald charge $2aB$.

In Fig. 3, we plotted the energy spectrum of accelerated particles in the MPP for the constant density profile of the accretion disk, $\sigma(r)$=const, and for the temperature profile

$$T(r) = r^{3/4} \left(1 - \sqrt{\frac{r_{\text{in}}}{r}}\right)^{1/4}, \tag{15}$$

where r_{in} is accretion disk inner edge. As we can see, the spectral index k for particle energy spectrum from Eq. 12 is now $k = 1.33$. A more complex model with both energy profile $E = E(r, \theta)$ and particle ionization profile $N = N(r, \theta)$ as a function of r and θ is given in as preliminary results Fig. 3 (right).

We assume the number density of accelerated high energy particles to be proportional to the total number density of particles in the accretion flow. The flux of high-energy particles escaping the vicinity of a black hole can be assumed to be proportional to the accretion rate of the black hole $\dot{M}$ if the particles are accelerated at the expense of the rotational energy of the black hole.

4 CONCLUSIONS

In this contribution, we have shown that SMBH in AGN can serve as the primary UHECR source. We calculate the distribution of accelerated particles in energy spaces, estimating the initial energetic spectral index k for the MPP one-shot acceleration model in the range $k \in (1, 3)$. Our initial injection spectrum is expected to change during the propagation of particles from the source to the detectors. More specific calculations of the spectrum taking into account energy losses and their effect on the spectral index for different possible CRs sources, including SMBH at the Galactic Center, are now in preparation.

ACKNOWLEDGEMENTS

This work was supported by Czech Science Foundation Grant (GAČR) No. 23-07043S. We also thank the internal grant of Silesian University, SGS/30/2023: Dynamics of structures in strong gravomagnetic fields of compact objects modeled in the framework of Einstein or alternative theories of gravity.

REFERENCES

Dadhich, N., Tursunov, A., Ahmedov, B. and Stuchlík, Z. (2018), The distinguishing signature of magnetic Penrose process, *Monthly Notices of the Royal Astronomical Society* , **478**(1), pp. L89–L94, arXiv: 1804.09679.

Frolov, V. P. and Shoom, A. A. (2010), Motion of charged particles near a weakly magnetized Schwarzschild black hole, *Phys. Rev. D* , **82**(8), 084034, arXiv: 1008.2985.

Kardashev, N. S. (1995), Cosmic supercollider, *Monthly Notices of the Royal Astronomical Society* , **276**(2), pp. 515–520.

Komissarov, S. S. (2022), Electrically charged black holes and the Blandford-Znajek mechanism, *Monthly Notices of the Royal Astronomical Society* , **512**(2), pp. 2798–2805, arXiv: 2108.08161.

Penrose, R. and Floyd, R. M. (1971), Extraction of Rotational Energy from a Black Hole, *Nature Physical Science*, **229**(6), pp. 177–179.

Rieger, F. M. (2022), Active Galactic Nuclei as Potential Sources of Ultra-High Energy Cosmic Rays, *Universe*, **8**(11), p. 607, arXiv: 2211.12202.

Stuchlík, Z. and Kološ, M. (2016), Acceleration of the charged particles due to chaotic scattering in the combined black hole gravitational field and asymptotically uniform magnetic field, *European Physical Journal C*, **76**, 32, arXiv: 1511.02936.

Tursunov, A. and Dadhich, N. (2019), Fifty Years of Energy Extraction from Rotating Black Hole: Revisiting Magnetic Penrose Process, *Universe*, **5**(5), p. 125, arXiv: 1905.05321.

Tursunov, A., Juraev, B., Stuchlík, Z. and Kološ, M. (2021), Electric Penrose process: High-energy acceleration of ionized particles by nonrotating weakly charged black hole, *Phys. Rev. D* , **104**(8), 084099, arXiv: 2109.10288.

Tursunov, A., Kološ, M. and Stuchlík, Z. (2022), Constraints on Cosmic Ray Acceleration Capabilities of Black Holes in X-ray Binaries and Active Galactic Nuclei, *Symmetry*, **14**(3), p. 482.

Tursunov, A., Stuchlík, Z. and Kološ, M. (2016), Circular orbits and related quasi-harmonic oscillatory motion of charged particles around weakly magnetized rotating black holes, *Phys. Rev. D* , **93**(8), 084012, arXiv: 1603.07264.

Tursunov, A., Stuchlík, Z., Kološ, M., Dadhich, N. and Ahmedov, B. (2020), Supermassive Black Holes as Possible Sources of Ultrahigh-energy Cosmic Rays, *The Astrophysical Journal* , **895**(1), 14, arXiv: 2004.07907.

Wagh, S. M., Dhurandhar, S. V. and Dadhich, N. (1985), Revival of the Penrose Process for Astrophysical Applications, *The Astrophysical Journal* , **290**, p. 12.

Wald, R. M. (1974), Black hole in a uniform magnetic field, *Phys. Rev. D* , **10**, pp. 1680–1685.

Zajaček, M., Tursunov, A., Eckart, A. and Britzen, S. (2018), On the charge of the Galactic centre black hole, *Monthly Notices of the Royal Astronomical Society* , **480**(4), pp. 4408–4423, arXiv: 1808.07327.